Effects of Different Guests on Pyrolysis Mechanism of A-CL-20/Guest at High Temperatures by Reactive Molecular Dynamics Simulations at High Temperatures

Mingming Zhou , Jing Luo , Dong Xiang *

Posted Date: 16 January 2023

doi: 10.20944/preprints202301.0260.v1

Keywords: host-guest inclusion strategy; pyrolysis decomposition; ReaxFF-MD; reaction rate

Article

Effects of Different Guests on Pyrolysis Mechanism of α-CL-20/Guest at High Temperatures by Reactive Molecular Dynamics Simulations at High Temperatures

Mingming Zhou, Jing Luo and Dong Xiang *

College of Chemistry and Environmental Engineering, Yangtze University, Jingzhou 434023, China; 2021720391@yangtzeu.edu.cn

* Correspondence: xiangdong@yangtzeu.edu.cn

Abstract: The host-guest inclusion strategy has potential to surpass the limitations of energy density and suboptimal performances of single explosives. The guest molecules can not only enhance the detonation performance of host explosives but can also enhance their stability. Therefore, the deeply analysis the role of guest influence on the pyrolysis decomposition of the host-guest explosive is necessary. The whole decomposition reaction stage of CL-20/H_2O, CL-20/CO_2, CL-20/N_2O, CL-20/NH_2OH was calculated by ReaxFF-MD. The incorporation of CO_2, N_2O and NH_2OH significantly increase the energy levels of CL-20. However, different guest has little influence on the initial decomposition paths of CL-20. The E_{a1} and E_{a2} values of CL-20/CO_2, CL-20/N_2O, CL-20/NH_2OH systems are higher than the CL-20/H_2O system. Clearly, incorporation of CO_2, N_2O, NH_2OH can inhibit the initial decomposition and intermediate decomposition stage of CL-20/H_2O. Guest molecules get heavily involved in the reaction and influence on the reaction rate. k_1 of CL-20/N_2O and CL-20/NH_2OH systems are significantly larger than that of CL-20/H_2O at high temperatures. k_1 of CL-20/CO_2 system is much complex, which can be affected deeply by temperatures. k_2 of CL-20/CO_2, CL-20/N_2O system is significantly smaller than that of CL-20/H_2O at high temperatures. k_2 of CL-20/NH_2OH system is little difference at high temperatures. For the CL-20/CO_2 system, the k_3 value of CO_2 is slight higher than that for CL-20/H_2O, CL-20/N_2O, CL-20/NH_2OH systems, while the k_3 values of N_2 and H_2O are slight smaller than that for CL-20/H_2O, CL-20/N_2O, CL-20/NH_2OH systems. For the CL-20/N_2O system, the k_3 value of CO_2 is slight smaller than that for CL-20/H_2O, CL-20/CO_2, CL-20/NH_2OH systems. For the CL-20/NH_2OH system, the k_3 value of H_2O is slight larger than that for CL-20/H_2O, CL-20/CO_2, CL-20/N_2O systems. These mechanisms revealed that CO_2, N_2O and NH_2OH molecules inhibit the early stages of the initial decomposition of CL-20, and play an important role for the decomposition subsequently.

Keywords: host-guest inclusion strategy; pyrolysis decomposition; ReaxFF-MD; reaction rate

1. Introduction

Successful balance between high energy and safety of energetic materials is challenging due to the time-consuming and difficult for synthesis of a new energetic materials. Host-guest energetic materials as shown in Figure 1 by embedding hydrogen-[1–3] or nitrogen-containing [4,5] oxidizing small molecules into the crystal lattice voids may be achieved highest possible energy density and the maximum possible chemical stability [6].

 doi:10.20944/preprints202301.0260.v1

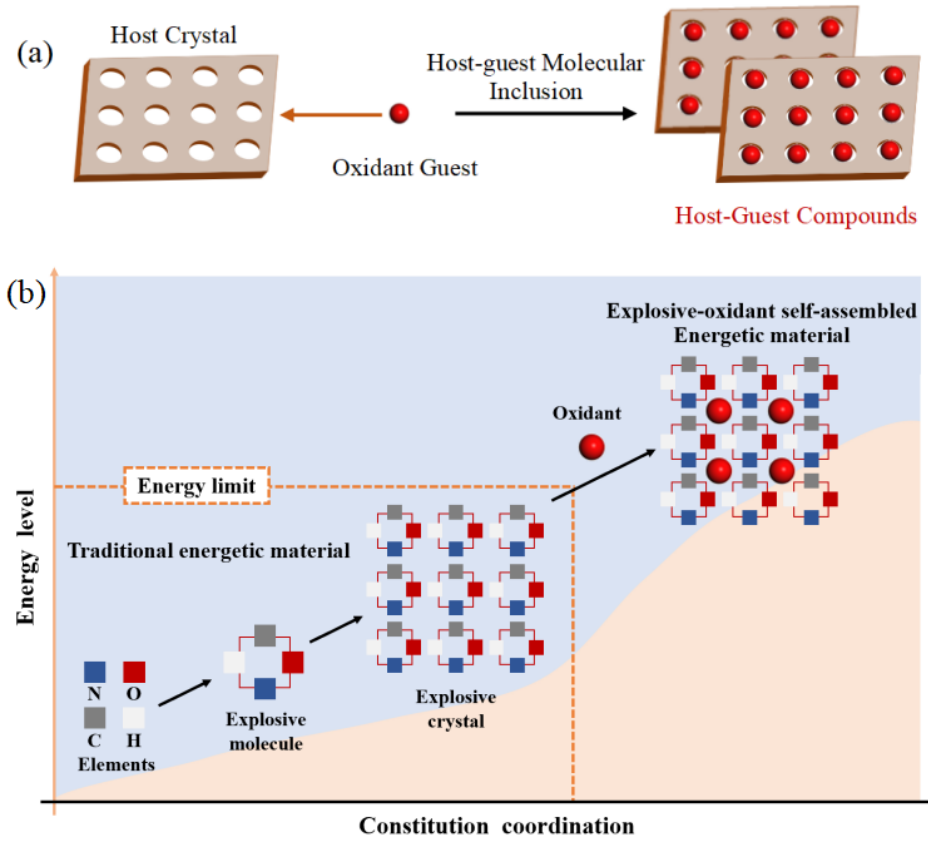

Figure 1. (a) 3D energetic host-guest inclusion materials [1]. (b) Illustration of explosive-oxidant self-assembled strategy and its comparison with traditional energetic material [2].

2,4,6,8,10,12-hexanitro-2,4,6,8,10,12-hexaazaisowurtzitane (CL-20) as one of the energetic materials with the highest density has been widely studied recently. Bennion J. C.[3] synthesized two polymorphic hydrogen peroxide (HP) solvates of α-CL-20. Two α-CL-20/H_2O_2 host-guest compounds are scarcely changing the lattice volume of the α-CL-20/H_2O and improving the energy. Thereafter, research focused on adopting a host-guest inclusion strategy to embed suitable guest within the void by removing water of α-CL-20/H_2O. A series of α-CL-20-guest energetic materials such as CL-20/CO_2[4], CL-20/N_2O [4], CL-20/NH_2OH [5] have been constructed in this manner.

The simulation of α-CL-20/guest mainly focused on the mechanism of host-guest molecular interaction and the pyrolysis mechanism at high temperatures. The intermolecular interaction is the central scientific issue of energetic cocrystals. Guo [6] had reviewed some typical energetic inclusion compounds and their structures, intermolecular interactions, stabilities, and energy properties. It provides a method to predict appropriate size of guest incorporate into the cavities of the α-CL-20 crystal. The systematically studies [7–9] on the comparison of interaction between the host-guest energetic complexes are devoted to summarizing the influence of guest on the performance of α-CL-20. The results would provide fundamental to summarize the properties of guest for α-CL-20/guest with structural stability. Meanwhile, in order to deeply analyze the role of hydrogen-guest small molecules in the host-guest system, the initial decomposition reactions of ICM-102/HNO_3[10], ICM-102/H_2O_2[11] with pure ICM-102 and CL-20/H_2O_2[12] at several high temperatures were systematically studied by molecular dynamics simulations. It was found that the addition of guest small molecules significantly increased the energy levels of ICM-102 and CL-20, but had little effect on the thermal stability of the host-guest system. The initial reaction path of ICM-102 molecule was not changed by HNO_3 and H_2O_2, but HNO_3 and H_2O_2 promoted the decomposition of ICM-102 molecule in the subsequent decomposition process. With the increase of temperature, the influence of H_2O_2 on the pyrolysis reaction of CL-20 weakens [13].

 doi:10.20944/preprints202301.0260.v1

All the simulation researches provide information to understand the influence of guest for the host explosives. However, the role of different nitrogen-guest small molecules in the host-guest system has not been studied systematically at different high temperatures. At the same high temperature, when do the different guest molecules participate in the decomposition reaction of host-guest explosive and how do they affect the decomposition process mechanism of host-guest explosive? What is the influence of the same guest on the pyrolysis of the host-guest explosive at different high temperatures? Therefore, detailed studies of the mechanism of the α-CL-20/nitrogen-guest detonation reaction at different high temperatures are necessary.

ReaxFF-MD [10,12,13] can conduct in-depth and detailed research on the pyrolysis mechanism of host-guest explosive at the microscopic scale, and find that how guest molecules participate in the pyrolysis reaction of the guest is an important factor affecting the energy release and detonation performance of the host explosives. In this study, we investigated the initial reaction of CL-20/CO_2, CL-20/N_2O, CL-20/NH_2OH and compared with the pure CL-20/H_2O at various temperatures (2500, 2750, 3000, 3250, and 3500K) by ReaxFF-lg reactive MD simulations (MD/ReaxFF-lg). The initial reaction paths, the change of generated/destroyed chemical bond numbers, the main product compositions, kinetic parameters in the different stages were analyzed. The mechanism for the improvement of the explosive energy and stability by incorporation of CO_2, N_2O and NH_2OH is also discussed.

2. Results and Discussion

2.1. Potential Energy (PE) and Total Energy for CL-20/H_2O, CL-20/CO_2, CL-20/N_2O, CL-20/NH_2OH Systems

The evolution of potential energy (PE) of CL-20/H_2O, CL-20/CO_2, CL-20/N_2O, CL-20/NH_2OH systems with time at (a) 2500K, (b) 2750K, (c) 3000K, (d) 3500K is shown in Figure 2. All the PE of CL-20/guest are much larger than that of CL-20/H_2O. It demonstrates that the addition of guest small molecules significantly increase the energy levels of CL-20 just shown in Figure 3. All the systems exhibit an initial rise in the PE curves at different temperatures which correspond to the endothermic reaction stage. When PE is maximized, the value thereafter decreases, signifying that the reaction becomes exothermic. The maximum value of PE increases in the order incorporation of $H_2O < NH_2OH < CO_2 < N_2O$ at different temperatures, and the heat release is also increased. That is, the incorporation of guests may have remarkable influence on heat release during the reaction. At a relatively low temperature of 2500K, the PE curve is smooth. However, when the temperature increase to 2750K, the PE curve is a little bit steeper. As the temperature increase to much higher 3000K and 3500K, the PE curve changed little. That is, no obvious heat release occurs during the reaction for much higher temperatures. With the increase of temperature, the PE observed to be close to equilibrium for much shorter time. Therefore, the higher the temperature, the earlier the complete reaction.

 doi:10.20944/preprints202301.0260.v1

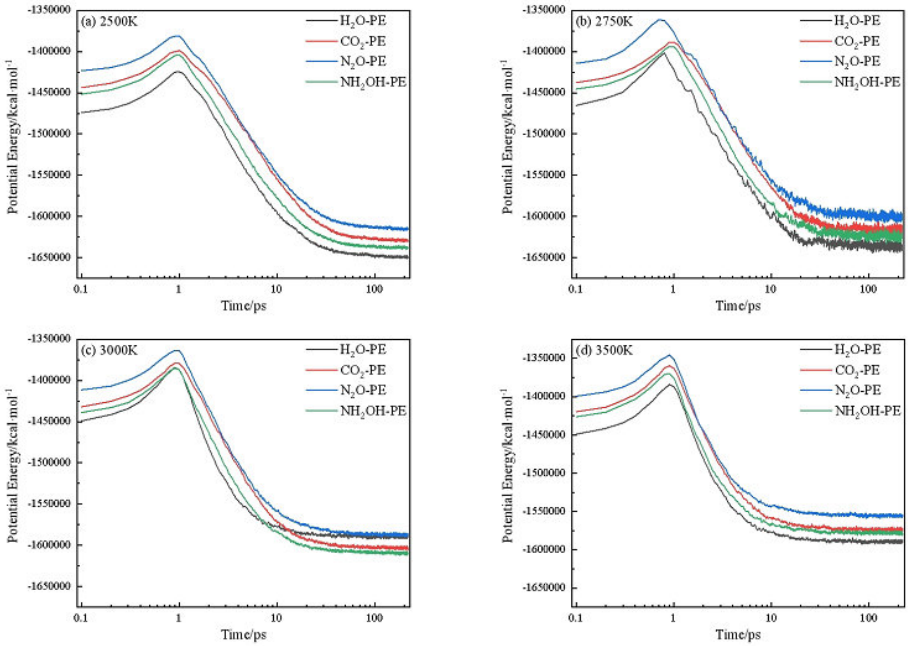

Figure 2. Evolution of potential energy of CL-20/H_2O, CL-20/CO_2, CL-20/N_2O, CL-20/NH_2OH system with time at (**a**) 2500K, (**b**) 2750K, (**c**) 3000K, (**d**) 3500K. Thick trendline corresponds to the actual concentration data of corresponding matching color.

The evolution of potential energy (PE) of (a) CL-20/H_2O, (b) CL-20/CO_2, (c) CL-20/N_2O, (d) CL-20/NH_2OH system with time at different temperatures is shown in Figure 3. The trend of PE curves for CL-20/H_2O and CL-20/N_2O is very similar. The trend of PE curves for CL-20/CO_2 and CL-20/NH_2OH is very similar. That is, the incorporation of N_2O may have the same influence on heat release with H_2O. While, the incorporation of CO_2 may have the same influence on heat release with NH_2OH.

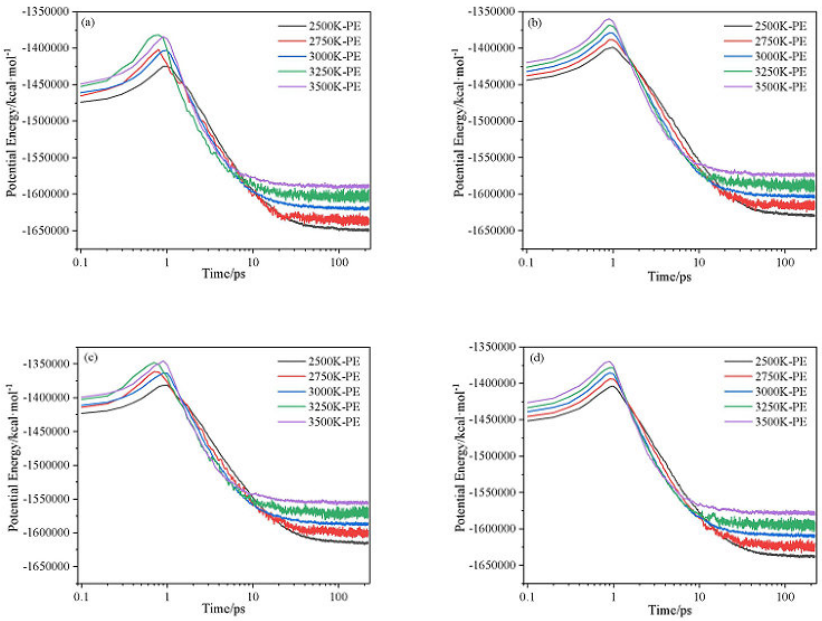

Figure 3. Evolution of potential energy of (a) CL-20/H_2O, (b) CL-20/CO_2, (c) CL-20/N_2O, (d) CL-20/NH_2OH system with time at different temperatures. Thick trendline corresponds to the actual concentration data of corresponding matching color.

 doi:10.20944/preprints202301.0260.v1

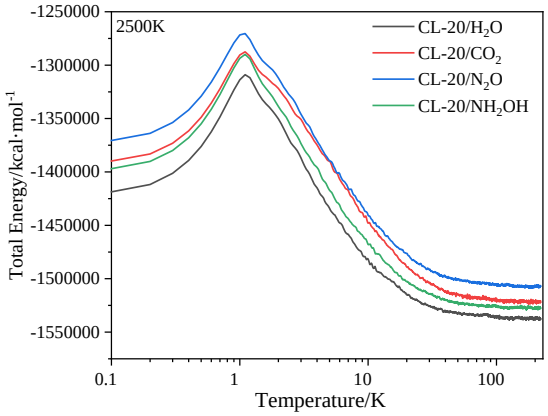

Figure 4. The total energy of CL-20/H_2O, CL-20/CO_2, CL-20/N_2O, CL-20/NH_2OH systems with time at 2500K. Thick trendline corresponds to the actual concentration data of corresponding matching color.

2.2. Initial Decomposition Stage

2.2.1. Initial Reaction Path of CL-20/Nitrogen-Guest

Table 1 shows the initial reaction paths of host-guest molecules and their occurrence frequency for CL-20/H_2O, CL-20/CO_2, CL-20/N_2O, CL-20/NH_2OH at four high temperatures. There are two main initial decomposition reactions of host CL-20 molecules $C_6H_6O_{12}N_{12} \longrightarrow C_6H_6O_{10}N_{11}+NO_2$ and $C_6H_6O_{12}N_{12} \longrightarrow C_6H_5O_{12}N_{12}+H$. The frequency of $C_6H_6O_{12}N_{12} \longrightarrow C_6H_6O_{10}N_{11}+NO_2$ is much more than that of $C_6H_6O_{12}N_{12} \longrightarrow C_6H_5O_{12}N_{12}+H$. As the increase with the temperatures, the frequency of both two main initial decomposition reaction improve for CL-20/H_2O, CL-20/CO_2, CL-20/N_2O, CL-20/NH_2OH. A small part of H_2O, N_2O, NH_2OH are broken to smaller pieces except for CO_2 with no decomposition. At the same high temperature, the frequency of both two main initial decomposition reactions are not significant difference for CL-20/H_2O, CL-20/CO_2, CL-20/N_2O, CL-20/NH_2OH. It demonstrates that different guest has little influence on the initial decomposition paths.

Table 1. The initial reaction paths of host-guest molecules and their occurrence frequency for CL-20/H_2O, CL-20/CO_2, CL-20/N_2O, CL-20/NH_2OH at four high temperatures.

Host-guest crystal	Temperatures	Initial reaction paths	Frequency
CL-20/H_2O	2500	$C_6H_6O_{12}N_{12} \rightarrow C_6H_6O_{10}N_{11}+NO_2$	29
		$C_6H_6O_{12}N_{12} \rightarrow C_6H_5O_{12}N_{12}+H$	21
		$H_2O \rightarrow H+OH$	20
	3000	$C_6H_6O_{12}N_{12} \rightarrow C_6H_6O_{10}N_{11}+NO_2$	51
		$C_6H_6O_{12}N_{12} \rightarrow C_6H_5O_{12}N_{12}+H$	31
		$H_2O \rightarrow H+OH$	20
	3500	$C_6H_6O_{12}N_{12} \rightarrow C_6H_6O_{10}N_{11}+NO_2$	69
		$C_6H_6O_{12}N_{12} \rightarrow C_6H_5O_{12}N_{12}+H$	41
		$H_2O \rightarrow H+OH$	27
CL-20/CO_2	2500	$C_6H_6O_{12}N_{12} \rightarrow C_6H_6O_{10}N_{11}+NO_2$	41
		$C_6H_6O_{12}N_{12} \rightarrow C_6H_5O_{12}N_{12}+H$	25
	3000	$C_6H_6O_{12}N_{12} \rightarrow C_6H_6O_{10}N_{11}+NO_2$	60
		$C_6H_6O_{12}N_{12} \rightarrow C_6H_5O_{12}N_{12}+H$	38
	3500	$C_6H_6O_{12}N_{12} \rightarrow C_6H_6O_{10}N_{11}+NO_2$	65
		$C_6H_6O_{12}N_{12} \rightarrow C_6H_5O_{12}N_{12}+H$	34
CL-20/N_2O	2500	$C_6H_6O_{12}N_{12} \rightarrow C_6H_6O_{10}N_{11}+NO_2$	30
		$C_6H_6O_{12}N_{12} \rightarrow C_6H_5O_{12}N_{12}+H$	25
		$N_2O \rightarrow N+NO$	5
		$N_2O \rightarrow N_2+O$	18

 doi:10.20944/preprints202301.0260.v1

	3000	$C_6H_6O_{12}N_{12}\rightarrow C_6H_6O_{10}N_{11}+NO_2$	63
		$C_6H_6O_{12}N_{12}\rightarrow C_6H_5O_{12}N_{12}+H$	31
		$N_2O\rightarrow N+NO$	5
		$N_2O\rightarrow N_2+O$	34
	3500	$C_6H_6O_{12}N_{12}\rightarrow C_6H_6O_{10}N_{11}+NO_2$	77
		$C_6H_6O_{12}N_{12}\rightarrow C_6H_5O_{12}N_{12}+H$	49
		$N_2O\rightarrow N+NO$	11
		$N_2O\rightarrow N_2+O$	24
	2500	$C_6H_6O_{12}N_{12}\rightarrow C_6H_6O_{10}N_{11}+NO_2$	31
		$C_6H_6O_{12}N_{12}\rightarrow C_6H_5O_{12}N_{12}+H$	22
		$NH_2OH\rightarrow NH_2+OH$	8
		$NH2OH\rightarrow NH_2O+H$	11
	3000	$C_6H_6O_{12}N_{12}\rightarrow C_6H_6O_{10}N_{11}+NO_2$	41
		$C_6H_6O_{12}N_{12}\rightarrow C_6H_5O_{12}N_{12}+H$	31
		$NH_2OH\rightarrow NH_2+OH$	27
$CL\text{-}20/NH_2OH$		$NH_2OH\rightarrow NH_2O+H$	15
	3500	$C_6H_6O_{12}N_{12}\rightarrow C_6H_6O_{10}N_{11}+NO_2$	69
		$C_6H_6O_{12}N_{12}\rightarrow C_6H_5O_{12}N_{12}+H$	48
		$C_6H_6O_{10}N_{11}\rightarrow C_6H_6O_8N_{10}+NO_2$	6
		$C_6H_5O_{12}N_{12}\rightarrow C_6H_5O_{10}N_{11}+NO_2$	7
		$C_6H_6O_{12}N_{12}\rightarrow C_6H_4O_{12}N_{12}+2H$	5
		$NH_2OH\rightarrow NH_2+OH$	35
		$NH_2OH\rightarrow NH_2O+H$	20

2.2.2. Effect of Nitrogen-Guest on the k_1

There are three stages for the evolution of the thermal decomposition of CL-20/nitrogen-guest. Firstly, the initial decomposition stage is characterized by rate constant k_1 and activation energy E_{a1}. Then, the intermediate decomposition stage is characterized by rate constant k_2 and activation energy E_{a2}. Finally, the final product evolution stage is characterized by rate constant k_3 and activation energy E_{a3}.

During the initial decomposition stage, the reaction rate was calculated by the change of the number of CL-20 molecules. The decay of the number of CL-20 molecules with time follows first-order decay exponential function [14]: $N(t) = N_0 \times \exp[-k_1(t - t_0)]$, where N_0 is the initial number of CL-20 molecules, t_0 is the time when CL-20 started to decompose, and k_1 is the initial decomposition stage rate constant (Table 2).

Table 2. Reaction rate constant k_1 in the initial endothermic reaction stage.

Host-guest crystal	T/K	k_1/ps^{-1}
$CL\text{-}20/H_2O$	2500	1.417
	2750	1.918
	3000	2.388
	3250	2.932
	3500	3.476
$CL\text{-}20/CO_2$	2500	1.179
	2750	1.745
	3000	2.131
	3250	3.075
	3500	3.984
$CL\text{-}20/N_2O$	2500	1.848
	2750	2.344
	3000	2.839
	3250	4.357
	3500	5.653
$CL\text{-}20/NH_2OH$	2500	1.434
	2750	2.163
	3000	2.851

 doi:10.20944/preprints202301.0260.v1

	3250	3.985
	3500	4.944

The logarithm of k_1 plotted against the inverse temperature (1/T) at 2500, 2750, 3000, 3250, and 3500 K is shown in Figure 5. The E_{a1} values of the CL-20/H_2O, CL-20/CO_2, CL-20/N_2O, CL-20/NH_2OH systems are 64.90, 87.12, 81.93 and 90.12 kJ·mol^{-1}, respectively. Clearly, incorporation of CO_2, N_2O, NH_2OH impede the initial decomposition. This indicates that nitrogen-guest can inhibit the trigger decomposition of CL-20/H_2O.

In addition, k_1 of CL-20/N_2O system is significantly larger than that of CL-20/H_2O at high temperatures. This indicates that N_2O significantly accelerates the reaction rate in the initial decomposition stage at high temperatures. k_1 of CL-20/NH_2OH system is significantly larger than that of CL-20/H_2O at relatively higher temperatures (3500K, 3250K, 3000K, 2750K). As the temperature decreased to 2500 K, the difference between k_1 of the CL-20/NH_2OH and CL-20/N_2O systems almost disappears. This indicates that NH_2OH significantly accelerates the reaction rate in the initial decomposition stage at relatively higher temperature. k_1 of CL-20/CO_2 system is much complex. At higher temperatures, k_1 of CL-20/CO_2 is much larger than that of CL-20/H_2O. However, k_1 of CL-20/CO_2 is much smaller than that of CL-20/H_2O at relatively lower temperatures. This indicates the temperature has significant influence on the initial decomposition rate for CL-20/CO_2.

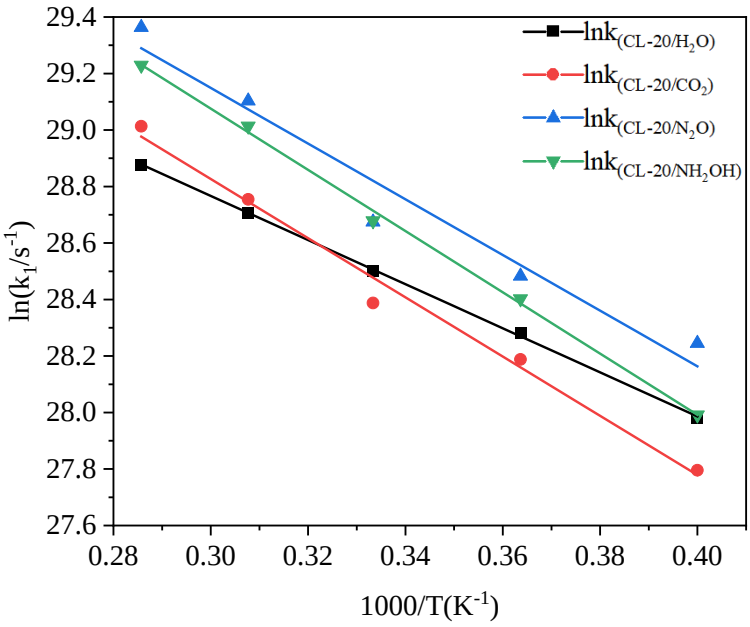

Figure 5. The logarithm of reaction rate (ln(k_1/s^{-1})) against inverse temperature (1/T) in the exothermic decomposition stage at different temperatures. Thick trendline corresponds to the actual concentration data of corresponding matching color.

2.3. Intermediate Decomposition Stage

2.3.1. Effect of Nitrogen-Guest on the Main Intermediate Products

Figure 6 shows the evolution curves of the main intermediate products and host-guest molecules at different temperatures. For CL-20/H_2O at 2500K, the number curve of host CL-20 fluctuates slightly, but the overall level remains horizontal before 0.5ps. The NO_2 fragments appears immediately at about 0ps. However, the number curve of guest H_2O fluctuates slightly, but the overall level remains horizontal before 0.9ps. This demonstrates that the initial decomposition of CL-20/H_2O may broken the C-NO_2 bonds of host CL-20 to form NO_2. During 0.5ps~1ps, the number of host CL-20 decreases sharply and disappears at 1ps, while the number of NO_2 fragments increases

 doi:10.20944/preprints202301.0260.v1

rapidly. During 0.9ps~1ps, the number of guest H_2O decreases, while the number of guest H_2O reaches the minimum value. It demonstrates that guest H_2O begins to participate the decomposition reaction deeply. The results of the trend are consistent with those of PE before 1ps for endothermic decomposition stage. During 0.5ps~1ps, the number of guest NO_2 increases sharply, while the number of guest NO_2 reaches the maximum value. Due to the participation of H_2O, the pyrolysis products begin to diversify. The NO_3 and NO fragments begin to appear. All the curves for NO_3 and NO fragments are similarity at the high temperatures. However, the amount of NO_3 and NO fragments would improve as the increase of temperatures. As the temperature increased, the variation curves of the main intermediate produces and host-guest molecules for CL-20/H_2O remains the same approximately. However, the reaction rates (k_2) are significantly different. The influence of high temperature on k_2 will analyse in the following section.

For CL-20/CO_2, CL-20/N_2O, CL-20/NH_2OH at high temperatures, the evolution tendency of the main intermediate products and host molecules is similar with that for CL-20/H_2O at 2500K. The variation curves of guest are quite different.

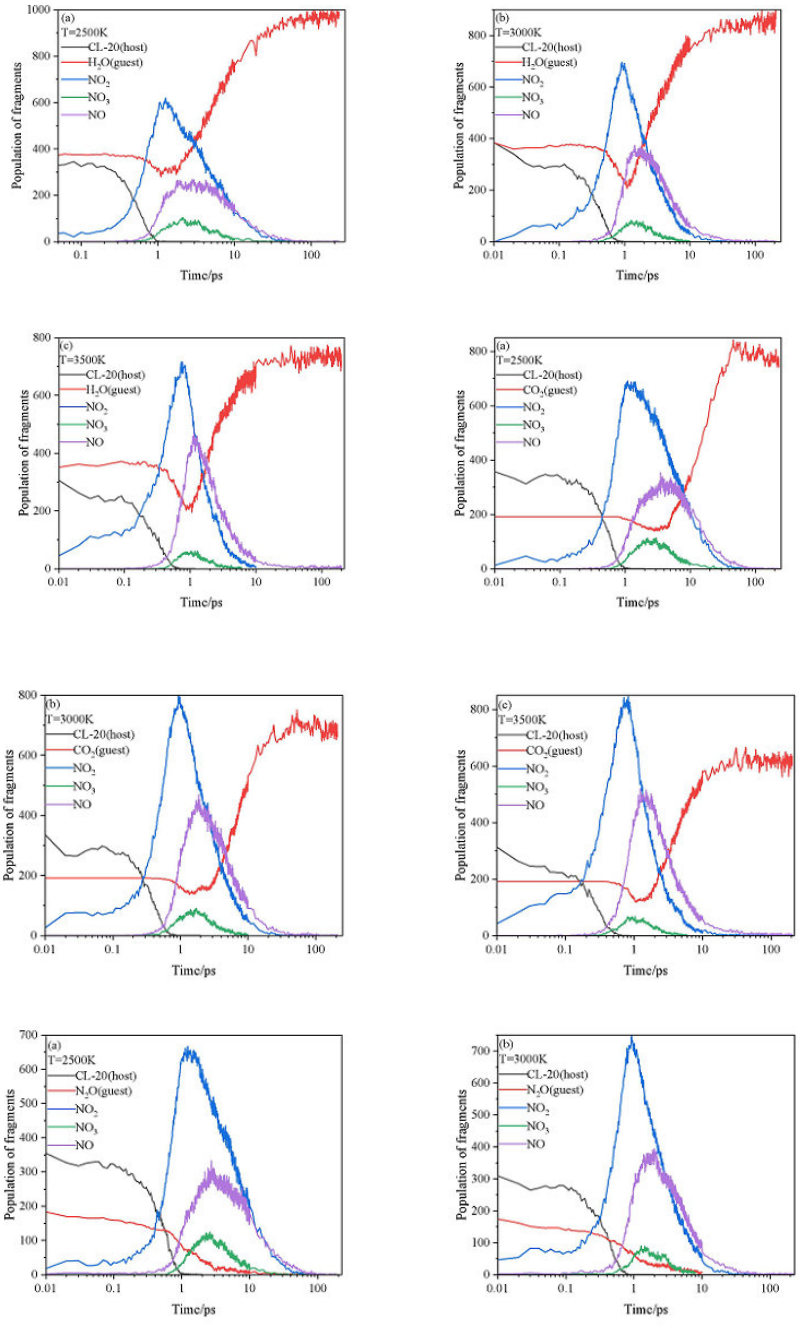

 doi:10.20944/preprints202301.0260.v1

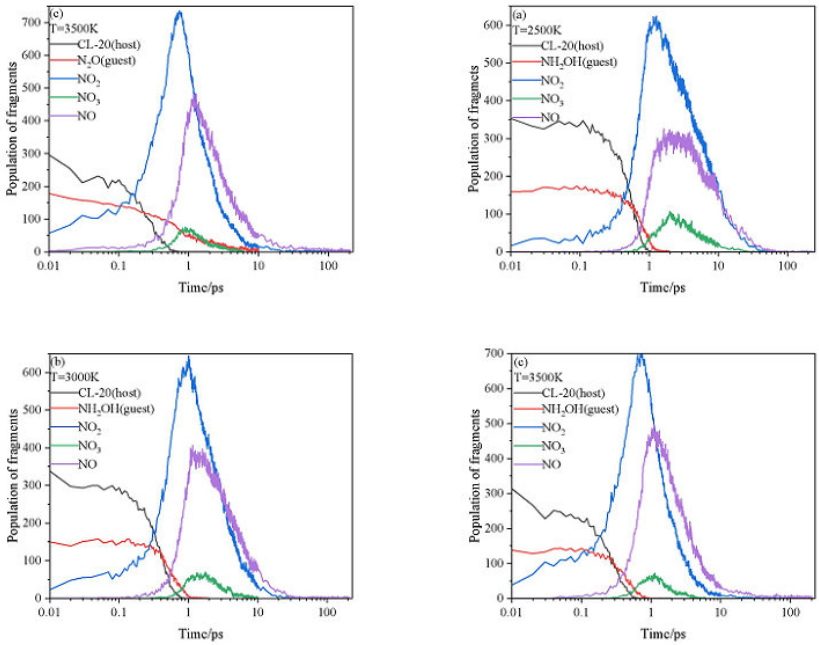

Figure 6. Evolution curves of the main intermediate products and host-guest molecules at different temperatures. Thick trendline corresponds to the actual concentration data of corresponding matching color.

Figures 7–9 show the evolution curves of the host and guest molecules for CL-20/H_2O, CL-20/CO_2, CL-20/N_2O, CL-20/NH_2OH at 2500K, 3000K, 3500K. All the host CL-20 variation tendency are similarity. The influence of different guest on k_2 is not significant at 2500K. With higher temperature, the k_2 significantly larger. The guest H_2O and CO_2, they are the main decomposition products. The variation tendency can divide into four stages: firstly, the tendency of guest is a level for little changeable. Secondly, it decreases for guest decomposition quickly. Then, it increase quickly as the main products. Finally, it reaches horizontal for the completely decomposition. There are two differences for the variation tendency: the first is that H_2O and CO_2 start to decrease at different times. The longer time to stay the first stage for CO_2 shows that CO_2 may be more stability than H_2O. And the second is that the minimum values of H_2O and CO_2 are different. It demonstrates that the more intense in pyrolysis reaction for H_2O than that of CO_2. As the increase of temperatures, the shorter time to stay the first stage and the smaller minimum for CO_2 and H_2O. It displays that the more intense in pyrolysis reaction at higher temperatures. For N_2O, NH_2OH just as the role for guest, the variation tendency slowly decreases and then sharply decreases until disappears. However, the reaction rates (k_2) for CO_2, N_2O, NH_2OH are significantly different at different temperatures.

 doi:10.20944/preprints202301.0260.v1

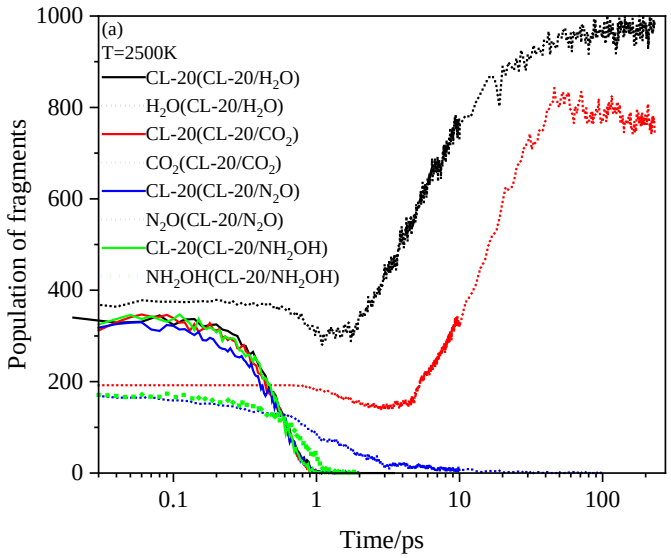

Figure 7. Evolution curves of the host and guest molecules for CL-20/H_2O, CL-20/CO_2, CL-20/N_2O, CL-20/NH_2OH at 2500K. Thick trendline corresponds to the actual concentration data of corresponding matching color.

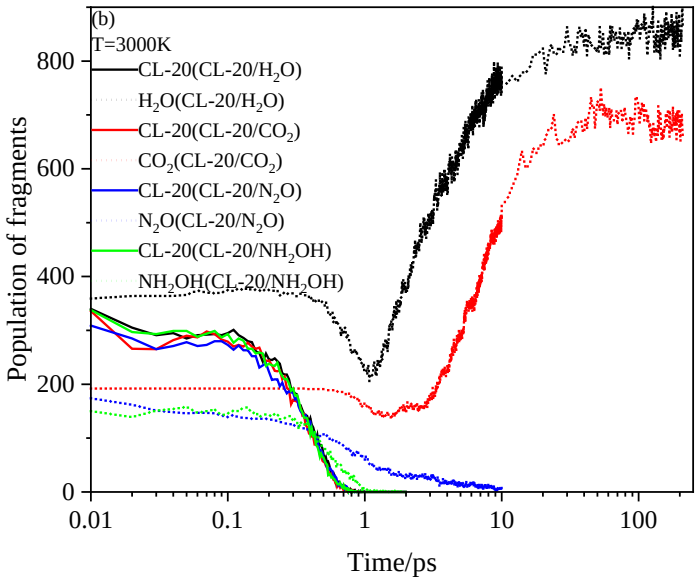

Figure 8. Evolution curves of the host and guest molecules for CL-20/H_2O, CL-20/CO_2, CL-20/N_2O, CL-20/NH_2OH at 3000K. Thick trendline corresponds to the actual concentration data of corresponding matching color.

 doi:10.20944/preprints202301.0260.v1

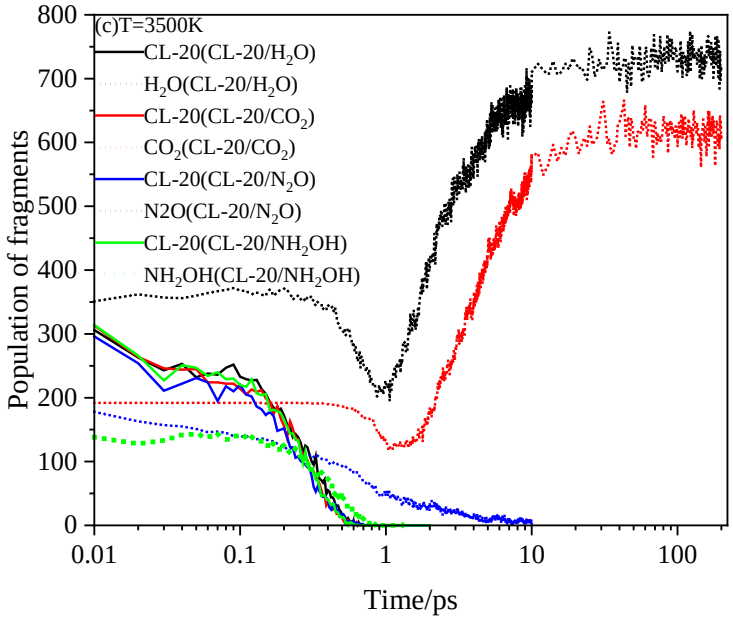

Figure 9. Evolution curves of the host and guest molecules for CL-20/H_2O, CL-20/CO_2, CL-20/N_2O, CL-20/NH_2OH at 3500K. Thick trendline corresponds to the actual concentration data of corresponding matching color.

2.3.2. Effect of Nitrogen-Guest on the k_2

After the PE reached the maximum value, the intermediate exothermic decomposition indicates the chemical reaction stage. The intermediate decomposition stage rate constant k_2 can be obtained by fitting the PE curves with a firstorder decay exponential function [15]: $U(t)=U_\infty+\Delta U_{exo}\bullet\exp[-k_2(t-t_{max})]$, where $U(t)$ is the potential energy value at time t, U_∞ is the asymptotic value of PE, ΔU_{exo} is the reaction heat, and its size is the difference between the maximun potential energy U_{max} and U_∞.

The chemical reaction rate constants obtained by fitting equation at different temperatures are shown in Table 3. The value of ΔU_{exo} has little change with the gradually increase of U_∞ and k_2 as temperature increase. This indicates that temperature has a limited effect on the exothermic reaction [16].

Table 3. Partial parameters of PE curve attenuation process.

Host-guest crystal	T/K	U_{max}	U_∞	ΔU_{exo}	k_2/ps^{-1}
	2500	-1424794	-1650929	226135	0.1523
	2750	-1413953	-1636452	222499	0.2251
CL-20/H_2O	3000	-1403193	-1621948	218755	0.2963
	3250	-1397567	-1606748	209181	0.38057
	3500	-1384266	-1591748	207482	0.46484
	2500	-1398845	-1630254	231409	0.11404
	2750	-1389461	-1617052	227591	0.17252
CL-20/CO_2	3000	-1379278	-1603764	224486	0.23059
	3250	-1369415	-1589817	220402	0.30645
	3500	-1359754	-1575870	216116	0.38217
	2500	-1381272	-1616532	235260	0.12789
	2750	-1372536	-1602557	230021	0.19377
CL-20/N_2O	3000	-1363624	-1588473	224849	0.25909
	3250	-1354660	-1572699	218039	0.35959
	3500	-1345497	-1556825	211328	0.46010
CL-20/NH_2OH	2500	-1403762	-1639940	236178	0.14567

 doi:10.20944/preprints202301.0260.v1

2750	-1395173	-1625769	230596	0.21743
3000	-1385384	-1611798	226414	0.28695
3250	-1377669	-1595917	218248	0.378106
3500	-1369830	-1580037	210207	0.47146

The logarithm of k_2 plotted against the inverse temperature (1/T) at 2500, 2750, 3000, 3250, and 3500 K is shown in Figure 10. The E_{a2} values of the CL-20/H_2O, CL-20/CO_2, CL-20/N_2O, CL-20/NH_2OH systems are 80.76, 87.58, 92.73 and 84.88 kJ·mol^{-1}, respectively. Clearly, incorporation of CO_2, N_2O, NH_2OH can inhibit the intermediate decomposition of CL-20/H_2O.

The pre-exponential factor derived from the pyrolysis simulations of the CL-20/H_2O, CL-20/CO_2, CL-20/N_2O, CL-20/NH_2OH systems are 29.65, 29.68, 30.03, 29.80. Assuming unimolecular decomposition, transition state theory leads to A = (k_BT/h)exp(ΔS/R) where $\Delta S_{(CL\text{-}20/H2O)}$=-17.47J•mol^{-1}•K^{-1}, $\Delta S_{(CL\text{-}20/CO2)}$=-17.23 J•mol^{-1}•K^{-1}, $\Delta S_{(CL\text{-}20/N2O)}$= -14.32J•mol^{-1}•K^{-1}, $\Delta S_{(CL\text{-}20/NH2OH)}$=-16.23J•mol^{-1}•K^{-1}. This negative activation of entropy is consistent with the TST for multimolecular reactions, suggesting that the reaction involves a multimolecular transition state [17]. The decrease of entropy at the transition state because of the embedding of nitrogen-containing guests.

In addition, k_2 of CL-20/CO_2 system is significantly smaller than that of CL-20/H_2O at high temperatures. This indicates that CO_2 significantly inhibits the reaction in the intermediate decomposition stage at high temperatures. k_2 of CL-20/N_2O system is significantly smaller than that of CL-20/H_2O at relatively lower temperatures (2500K and 2750K). As the temperature increased to 3500 K, the difference between k_2 of the CL-20/H_2O and CL-20/N_2O systems almost disappears. This indicates that N_2O significantly restrains the reaction in the intermediate decomposition stage at relatively low temperature. With increasing temperature, N_2O has increasingly less effect on the reaction rate. However, k_1 of CL-20/N_2O indicates that N_2O significantly accelerates the reaction in the initial decomposition stage at high temperatures. The conclusion is contrary to that for ICM-102/HNO_3[18]. This maybe caused by the hydrogen content for nitrogen-guest. k_2 of CL-20/H_2O and CL-20/NH_2OH systems are little difference at high temperatures, NH_2OH has little effect on the reaction rate at high temperatures. The opposite effect of CL-20/H_2O_2[19] maybe due to the difference of hydrogen content in the guest. The influence of CO_2 and N_2O on the decomposition reaction of host explosive may be the little interaction between CO_2, N_2O and CL-20[20]. However, the influence of H_2O_2 on the decomposition reaction of host explosive may be the significant interaction between H_2O_2 and CL-20 [20].

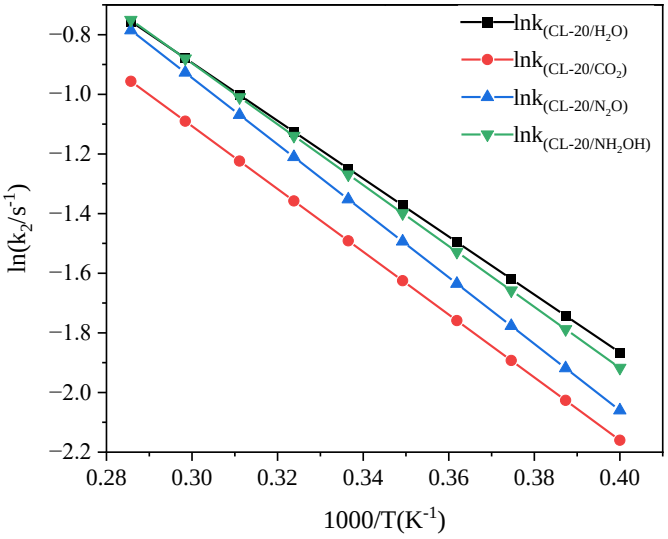

Figure 10. The logarithm of reaction rate (ln(k_1/s^{-1})) against inverse temperature (1/T) in the exothermic decomposition stage at different temperatures. Thick trendline corresponds to the actual concentration data of corresponding matching color.

 doi:10.20944/preprints202301.0260.v1

2.4. Final Product Evolution Stage

2.4.1. Effect of Nitrogen-Guest on the Final Products

To clarify the effect of CO_2, N_2O and NH_2OH molecules on the main products, the population of CO_2, N_2, H_2O after the complete decomposition reaction for CL-20/H_2O, CL-20/CO_2, CL-20/N_2O, CL-20/NH_2OH at 2500K, 3000K and 3500K are shown at Figures 11–13.

The population of CO_2 for CL-20/NH_2OH and CL-20/H_2O are nearly equivalent at high temperatures. The population of CO_2 for CL-20/N_2O is the lowest, while the population of CO_2 for CL-20/H_2O is largest at 2500K. As the temperature increase, the more population of CO_2 for CL-20/N_2O grows acutely. However, the population of CO_2 for CL-20/CO_2, CL-20/NH_2OH decrease acutely. It demonstrates that the CO_2 produced mechanism for N_2O guest is different with CO_2 and NH_2OH guests. The population of N_2 for CL-20/NH_2OH and CL-20/H_2O are nearly equivalent at high temperatures. As the temperature increase, the more population of CO_2 for CL-20/CO_2, CL-20/N_2O grows acutely. It demonstrates that the N_2 produced mechanism for NH_2OH guest is different with CO_2 and N_2O guests. The population of H_2O for CL-20/NH_2OH and CL-20/H_2O are nearly equivalent at high temperatures. The population of H_2O for CL-20/CO_2 and CL-20/N_2O are nearly equivalent at high temperatures. The variation tendency of population for three main products shows that the influence of guest NH_2OH and H_2O, CO_2 and N_2O are much same to each other. This may be caused by the hydrogen for two group guest.

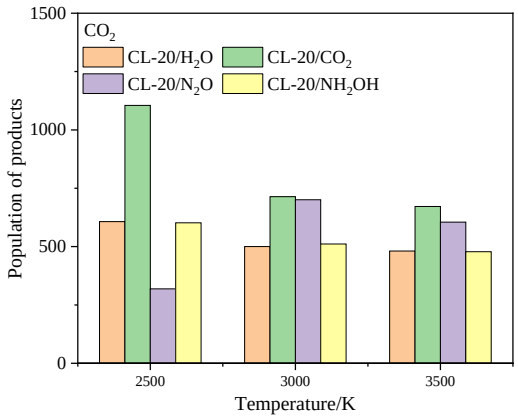

Figure 11. The population of CO_2 after the complete decomposition reaction for CL-20/H_2O, CL-20/CO_2, CL-20/N_2O, CL-20/NH_2OH at 2500K, 3000K and 3500K.

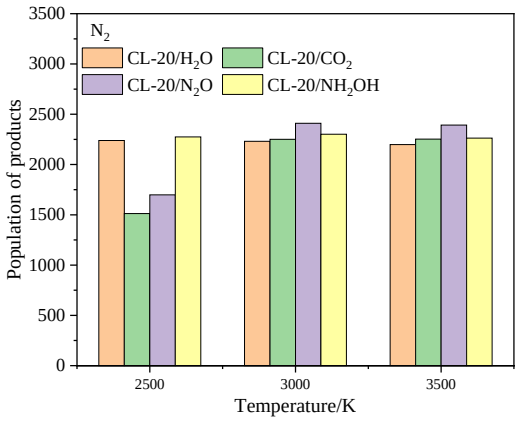

Figure 12. The population of N_2 after the complete decomposition reaction for CL-20/H_2O, CL-20/CO_2, CL-20/N_2O, CL-20/NH_2OH at 2500K, 3000K and 3500K.

 doi:10.20944/preprints202301.0260.v1

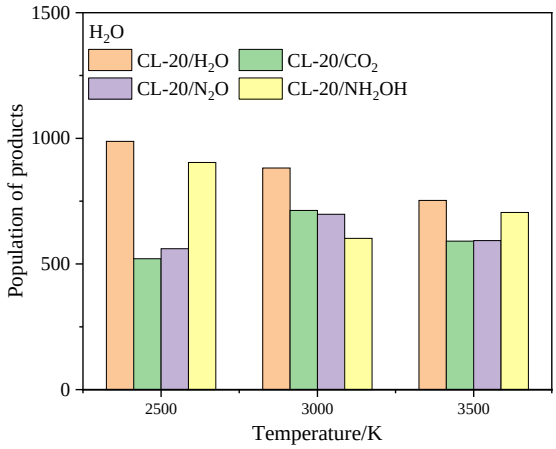

Figure 13. The population of H_2O after the complete decomposition reaction for CL-20/H_2O, CL-20/CO_2, CL-20/N_2O, CL-20/NH_2OH at 2500K, 3000K and 3500K.

2.4.2. Effect of Nitrogen-Guest on the k_3

The final products of thermal decomposition of CL-20/guest are N_2, CO_2 and H_2O. The formation rates k_3 can be obtained by fitting the variation trend of the final products with the exponential function [21]: $C(t)= C_\infty\{1-\exp[-k_3(t-t_i)]\}$, where C_∞ is the asymptotic number of the product, k_3 is the formation rate constant of the product, and t_i is the time of appearance of the product.

Comparison of the k_3 values of CO_2, H_2O and N_2 for the (a) CL-20/H_2O, (b) CL-20/CO_2, (c) CL-20/N_2O, (d) CL-20/NH_2OH at different temperatures is shown in Figure 14. All the k_3 values of CO_2, H_2O and N_2 are increased as the temperature improvement. This may be due to the facilitation on production the three main products. The k_3 values of H_2O is larger than that of N_2 , while the k_3 values of N_2 is larger than that of CO_2 for CL-20/H_2O, CL-20/CO_2, CL-20/N_2O, CL-20/NH_2OH. This demonstrates that the production of H_2O is the easiest and the production of CO_2 is the least.

 doi:10.20944/preprints202301.0260.v1

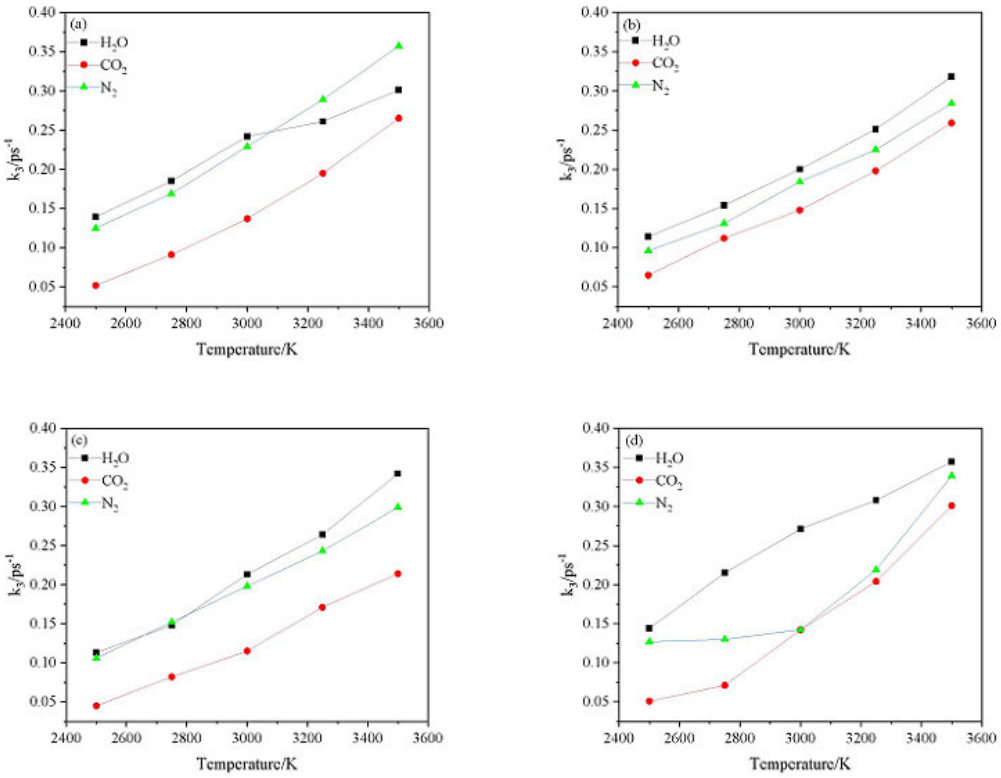

Figure 14. Comparison of the k_3 values of CO_2, H_2O and N_2 for (a) CL-20/H_2O, (b) CL-20/CO_2, (c) CL-20/N_2O, (d) CL-20/NH_2OH at different temperatures. Thick trendline corresponds to the actual concentration data of corresponding matching color.

Comparison of the k_3 values of CO_2, H_2O and N_2 for the CL-20/H_2O, CL-20/CO_2, CL-20/N_2O, CL-20/NH_2OH at different temperatures is shown in Figure 15. For the CL-20/CO_2 system, the k_3 value of CO_2 is slight higher than that for CL-20/H_2O, CL-20/N_2O, CL-20/NH_2OH systems, while the k_3 values of N_2 and H_2O are slight smaller than that for CL-20/H_2O, CL-20/N_2O, CL-20/NH_2OH systems. This indicates that CO_2 restrains the formation of H_2O and N_2 molecules. For the CL-20/N_2O system, the k_3 value of CO_2 is slightly smaller than that for CL-20/H_2O, CL-20/CO_2, CL-20/NH_2OH systems. This indicates that N_2O restrains the formation of CO_2. For the CL-20/NH_2OH system, the k_3 value of H_2O is slightly larger than that for CL-20/H_2O, CL-20/CO_2, CL-20/N_2O systems. This indicates that NH_2OH accelerates the formation of H_2O.

 doi:10.20944/preprints202301.0260.v1

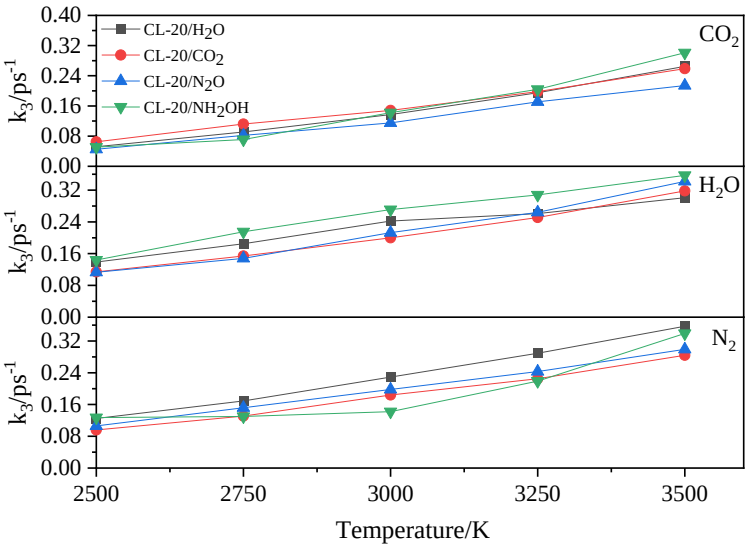

Figure 15. Comparison of the k_3 values of CO_2, H_2O and N_2 for CL-20/H_2O, CL-20/CO_2, CL-20/N_2O, CL-20/NH_2OH at different temperatures. Thick trendline corresponds to the actual concentration data of corresponding matching color.

3. Discussion

We have performed MD/ReaxFF-lg simulations to investigate the thermal decomposition reaction of the CL-20/H_2O, CL-20/CO_2, CL-20/N_2O, CL-20/NH_2OH systems at different temperatures. In this work, guest is not only enhanced the safety but also improved its detonation performance.

During the thermal decomposition reaction of CL-20/H_2O, CL-20/CO_2, CL-20/N_2O, CL-20/NH_2OH systems at different temperatures, the initial reaction path is not significantly influenced by the incorporation of CO_2, N_2O, NH_2OH: $C_6H_6O_{12}N_{12} \longrightarrow C_6H_6O_{10}N_{11}+NO_2$ and $C_6H_6O_{12}N_{12} \longrightarrow C_6H_5O_{12}N_{12}+H$. At the same high temperature, the frequency of both two main initial decomposition reaction are not significant difference for CL-20/H_2O, CL-20/CO_2, CL-20/N_2O, CL-20/NH_2OH. As the increase with the temperatures, the frequency of both two main initial decomposition reaction improve for CL-20/H_2O, CL-20/CO_2, CL-20/N_2O, CL-20/NH_2OH. The nitrogen-guest can inhibit the trigger decomposition for the larger E_{a1} and E_{a2} values. By embedding N_2O and NH_2OH can significantly accelerate the reaction in the initial decomposition rates at high temperatures for the larger k_1 at high temperatures. However, incorporation of CO_2, higher temperature has significant influence on the initial decomposition for the complex k_1. By embedding CO_2 and N_2O significantly inhibits the reaction in the intermediate decomposition stage at high temperatures for the smaller k_2 at high temperatures. Incorporation of NH_2OH has little effect on the reaction rate at high temperatures with the little difference of k_2. All the k_3 values of CO_2, H_2O and N_2 are increased as the temperature improvement. Guest CO_2 restrains the formation of H_2O and N_2 molecules for the higher k_3 value. Guest N_2O restrains the formation of CO_2 for the higher k_3 value. Guest NH_2OH accelerates the formation of H_2O molecules for the higher k_3 value. The influence of guest NH_2OH and H_2O, N_2O and CO_2 on decomposition products maybe similarity for the same amount products with each other.

The results of this study revealed that the guest CO_2, N_2O and NH_2OH played a certain inhibitory role during the early stages of the host CL-20 thermal decomposition reaction. The study provided a theoretical basis for the synthesis of new energetic materials with host-guest inclusion strategy.

 doi:10.20944/preprints202301.0260.v1

4. Computational Methods

The initial unit cell structures of CL-20/H_2O, CL-20/CO2, CL-20/N_2O and CL-20/NH_2OH were obtained from the Cambridge Crystallographic Data Centre. In the unit cell, there are eight CL-20 molecules and four guest molecules (H_2O, CO_2, N_2O and NH_2OH) (Figure 16). We enlarged the unit cell 48 times along both the *a*, the *b* and *c* axes to construct a 6*4*2 supercell containing 48 unit cells ((a) contain 384 of CL-20 and 384 of guest. The supercell of (b), (c), (d) contains 384 of CL-20 and 192 of guest).

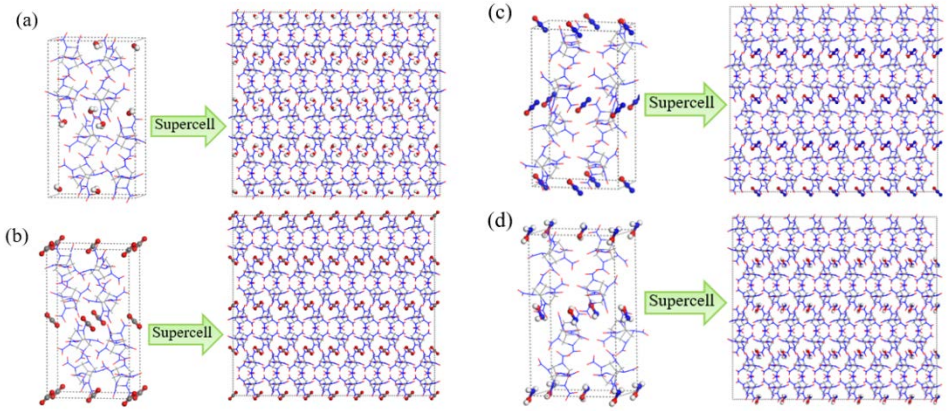

Figure 16. (a) α-CL-20/H_2O, 6*4*2 α-CL-20/H_2O supercell, (b) α-CL-20/CO_2, 6*4*2 α-CL-20/CO_2 supercell, (c) α-CL-20/N_2O, 6*4*2 α-CL-20/N_2O supercell, (d) α-CL-20/NH_2OH, 6*4*2 α-CL-20/NH_2OH supercell. The blue atoms represent nitrogen, the red atoms represent oxygen, the white atoms represent hydrogen, the gray atoms represent carbon. The supercell of (a) contain 384 of CL-20 and 384 of guest. The supercell of (b), (c), (d) contains 384 of CL-20 and 192 of guest.

First, the canonical ensemble (NVT) and the Berendsen thermostat were applied to the molecular dynamics (MD) simulation with a total time of 10 ps at 1 K, which further relaxed the α-CL-20/guest supercell. Then, ReaxFF-lg isobaric-isothermal MD (NPT-MD) simulations were performed for 5 ps at 300K controlled by the Berendsen thermostat based on the relax supercell. To instantaneously heat the system from 300 K with NVT-MD simulations to the target temperatures (2500, 2750, 3000, 3250, and 3500 K) to ensure the accuracy of the fitted reaction rate constant and activation energy, we set the damping constant to 0.25 fs. Komeiji demonstrated that 0.25 fs is enough for calculation accuracy of bonds and angles in molecular dynamics simulations. NVT-MD simulations of the supercell system with the Berendsen thermostat were performed until the potential energy (PE) stabilized. An analysis of the fragments was performed with a 0.3 bond order cutoff value for each atom pair to identify the chemical species [22,23]. The information of the dynamic trajectory was recorded every 20 fs, which was used to analyze the evolution details of α-CL-20/guest in the pyrolysis process.

To verify the suitability of the ReaxFF-lg force field for the CL-20/guest system, we compared the lattice parameters and density of relaxed CL-20/guest at 298 K and 0 Pa with the initial structure from the CCDC (Table 4). The cell parameters and density of relaxed CL-20/guest calculated by MD/ReaxFF-lg agreed well with the initial structure values for the error value < 5%. This preliminarily indicated that ReaxFF-lg can describe the decomposition of CL-20/guest system.

Table 4. Comparison of lattice parameters and density of CL-20/guest.

Crystal	Method	*a*/Å	*b*/Å	*c*/Å	ρ/g·cm^{-3}
CL-20/H_2O	from CCDC	9.477	13.139	23.380	2.081
	ReaxFF-lg	9.370	12.993	23.119	2.153
CL-20/CO_2	from CCDC	9.673	13.203	23.553	2.033
	ReaxFF-lg	9.467	13.167	23.489	2.049
CL-20/N_2O	from CCDC	9.577	13.256	23.625	2.038
	ReaxFF-lg	9.427	13.049	23.256	2.137

CL-20/NH_2OH	from CCDC	9.789	13.123	23.509	2.000
	ReaxFF-lg	9.602	12.873	23.059	2.119

Author Contributions: Investigation, M.Z.; data curation, M.Z. and J.L.; writing—original draft preparation, M.Z. and D.X.; writing—review and editing, D.X.; supervision, D.X. All authors have read and agreed to the published version of the manuscript.

Funding: This research was funded by the Provincial Science Foundation of Hubei (Grant No. 2022CFB634) and Provincial Science Foundation of Xinjiang (Grant No. 2022D01A329).

Institutional Review Board Statement: Not applicable.

Informed Consent Statement: Not applicable.

Conflicts of Interest: The authors declare no conflict of interest.

References

1. Wang, Y., Song, S., Huang, C., Qi, X., Wang, K., Liu, Y., Zhang, Q. Hunting for advanced high-energy-density materials with well-balanced energy and safety through an energetic host-guest inclusion strategy. J. Mater. 2019, 7(33), 19248-19257. https://doi.org/10.1039/C9TA04677A.
2. Song, S., Wang, Y., He, W., Wang, K., Yan, M., Yan, Q., Zhang, Q. Melamine n-oxide based self-assembled energetic materials with balanced energy & sensitivity and enhanced combustion behavior. Chem. Eng. J. 2020, 395, 125114. https://doi.org/10.1016/j.cej.2020.125114.
3. Bennion, J. C., Chowdhury, N., Kampf, J. W., Matzger, A. J. Hydrogen peroxide solvates of 2, 4, 6, 8, 10, 12-hexanitro-2, 4, 6, 8, 10, 12-hexaazaisowurtzitane. Angew. 2016, 128(42), 13312-13315. https://doi.org/10.1002/ange.201607130.
4. Xu, J., Zheng, S., Huang, S., Tian, Y., Liu, Y., Zhang, H., Sun, J. Host–guest energetic materials constructed by incorporating oxidizing gas molecules into an organic lattice cavity toward achieving highly-energetic and low-sensitivity performance. ChemComm. 2019, 55(7), 909-912. https://doi.org/10.1039/C8CC07347C.
5. Sun, S., Zhang, H., Wang, Z., Xu, J., Huang, S., Tian, Y., Sun, J. Smart host–guest energetic material constructed by stabilizing energetic fuel hydroxylamine in lattice cavity of 2,4,6,8,10,12-hexanitrohexaazaisowurtzitane significantly enhanced the detonation, safety, propulsion, and combustion performances. ACS. Appl. Mater. Interfaces. 2021, 13(51), 61324-61333. https://doi.org/10.1021/acsami.1c20859.
6. Guo, Z., Wang, Y., Zhang, Y., Ma, H. Energetic host-guest inclusion compounds: an effective design paradigm for high-energy materials. CrystEngComm. 2022, 24, 3667-3674. https://doi.org/10.1039/D2CE00171C.
7. Liu, G., Wei, S. H., Zhang, C. Review of the intermolecular interactions in energetic molecular cocrystals. Cryst. Growth. Des. 2020, 20(10), 7065-7079. https://doi.org/10.1021/acs.cgd.0c01097.
8. Zhao, X., Huang, S., Liu, Y., Li, J., Zhu, W. Effects of noncovalent interactions on the impact sensitivity of hns-based cocrystals: a DFT study. Cryst. Growth. Des. 2018, 19(2), 756-767. https://doi.org/10.1021/acs.cgd.8b01334.
9. Wang, K., Zhu, W. Insight into the roles of small molecules in CL-20 based host-guest crystals: a comparative DFT-D study. CrystEngComm. 2020, 22(37), 6228-6238. https://doi.org/10.1039/D0CE00853B.
10. Xiao, Y., Chen, L., Yang, K., Geng, D., Lu, J., Wu, J. Mechanism of the improvement of the energy of host-guest explosives by incorporation of small guest molecules: HNO_3 and H_2O_2 promoted C–N bond cleavage of the ring of ICM-102. Sci. Rep. 2021, 11(1), 1-12. https://doi.org/10.21203/rs.3.rs-294160/v1.
11. Xiao, Y., Chen, L., Geng, D., Yang, K., Lu, J., Wu, J. A quantum-based molecular dynamics study of the ICM-102/HNO_3 host-guest reaction at high temperatures. Phys. Chem. Chem. Phys. 2020, 22(46), 27002-27012. https://doi.org/10.1039/D0CP04511J.
12. Xiao, Y., Chen, L., Geng, D., Yang, K., Lu, J., Wu, J., Yu, B. Reaction mechanism of embedding oxidizing small molecules in energetic materials to improve the energy by reactive molecular dynamics simulations. J. Phys. Chem. C. 2019, 123(48), 29144-29154. https://doi.org/10.1021/acs.jpcc.9b09070.
13. Zhang, L., Jiang, S. L., Yu, Y., Chen, J. Revealing solid properties of high-energy-density molecular cocrystals from the cooperation of hydrogen bonding and molecular polarizability. Sci. Rep. 2019, 9(1), 1-7. https://doi.org/10.1038/s41598-018-37500-y.
14. Rom, Naomi., Zybin, Sergey. V., van, Duin., Adri, C. T., Goddard, William. A., Zeiri, Yehuda., Katz, Gil., Kosloff, Ronnie. Density-dependent liquid nitromethane decomposition: molecular dynamics simulations based on ReaxFF. J. Phys. Chem. A. 2011, 115(36), 10181–10202. https://doi.org/10.1021/jp202059v.
15. Wang, F., Chen, L., Geng, D., Wu, J., Lu, J., Wang, C. Thermal decomposition mechanism of CL-20 at different temperatures by ReaxFF reactive molecular dynamics simulations. J. Phys. Chem. A. 2018, 122(16), 3971-3979. https://doi.org/10.1021/acs.jpca.8b01256.

16. Zhang, L., Zybin, S. V., Van Duin, A. C., Dasgupta, S., Goddard III, W. A., Kober, E. M. Carbon cluster formation during thermal decomposition of octahydro-1, 3, 5, 7-tetranitro-1, 3, 5, 7-tetrazocine and 1, 3, 5-triamino-2, 4, 6-trinitrobenzene high explosives from ReaxFF reactive molecular dynamics simulations. J. Phys. Chem. A. 2009, 113(40), 10619-10640. https://doi.org/10.1021/jp901353a.
17. Liu, L., Bai, C., Sun, H., Goddard III, W. A. Mechanism and kinetics for the initial steps of pyrolysis and combustion of 1, 6-dicyclopropane-2, 4-hexyne from ReaxFF reactive dynamics. J. Phys. Chem. A. 2021, 115(19), 4941-4950. https://doi.org/10.1021/jp110435p.
18. Xiao, Y., Chen, L., Geng, D., Yang, K., Lu, J., Wu, J., Yu, B. Reaction mechanism of embedding oxidizing small molecules in energetic materials to improve the energy by reactive molecular dynamics simulations. J. Phys. Chem. C. 2019, 123(48), 29144-29154. https://doi.org/10.1021/acs.jpcc.9b09070.
19. Xiao, Y., Chen, L., Geng, D., Yang, K., Lu, J., Wu, J., Yu, B. Reaction mechanism of embedding oxidizing small molecules in energetic materials to improve the energy by reactive molecular dynamics simulations. *J. Phys. Chem. C*. 2019, *123*(48), 29144-29154. https://doi.org/10.1021/acs.jpcc.9b09070.
20. Zhou, M., Ye, C., Xiang, D. Theoretical studies on the role of guest in α-CL-20/guest crystals. Molecules. 2022, 27(10), 3266. https://doi.org/10.3390/molecules27103266.
21. Bai, H., Gou, R., Chen, M., Zhang, S., Chen, Y., Hu, W. ReaxFF/lg molecular dynamics study on thermal decomposition mechanism of 1-methyl-2, 4, 5-trinitroimidazole. Comput. Theor. Chem. 2022, 1209, 113594. https://doi.org/10.1016/j.comptc.2022.113594.
22. Strachan, A., van Duin, A. C., Chakraborty, D., Dasgupta, S., Goddard III, W. A. Shock waves in high-energy materials: The initial chemical events in nitramine RDX. Phys. Rev. Lett. 2003, 91(9), 098301. https://doi.org/10.1103/PhysRevLett.91.098301.
23. Strachan, A., Kober, E. M., Van Duin, A. C., Oxgaard, J., Goddard III, W. A. Thermal decomposition of RDX from reactive molecular dynamics. J. Chem. Phys. 2005, 122(5), 054502. https://doi.org/10.1063/1.1831277.